

# Preliminary Results From Nighttime Lights Change Detection

C.D. Elvidge<sup>a,\*</sup>, K.E. Baugh<sup>b</sup>, J. Safran<sup>b</sup>, B.T. Tuttle<sup>b</sup>, A.T. Howard<sup>b</sup>, P.J. Hayes<sup>b</sup>, J. Jantzen<sup>b</sup>, E.H. Erwin<sup>a</sup>

<sup>a</sup> NOAA National Geophysical Data Center, Boulder, Colorado 80305 USA - (chris.elvidge and edward.h.erwin@noaa.gov)

<sup>b</sup> Cooperative Institute for Environmental Research, University of Colorado, Boulder, Colorado 80303 USA

**KEY WORDS:** Nighttime lights, change detection, sprawl development

## ABSTRACT:

The Defense Meteorological Satellite Program (DMSP) Operational Linescan System (OLS) has a unique capability to collect low-light imaging data of the earth at night. The OLS and its predecessors have collected this style of data on a nightly global basis since 1972. The digital archive of OLS data extends back to 1992. Over the years several global nighttime lights products have been generated. NGDC has now produced a set of global cloud-free nighttime lights products, specifically processed for the detection of changes in lighting emitted by human settlements, spanning 1992-93 to 2003. While OLS data leave much to be desired for urban remote sensing (coarse spatial resolution - 2.7 km ground sample distance, limited dynamic range - 6 bit quantization and no on-board calibration) significant changes in lighting can be observed in the change pair: rings of growth in lighting surround many urban centers, suites of linear features found in countries such as United Arab Emirates and China, and the contraction of lighting across much of the former Soviet Union. A major issue affecting the use of the time series in change detection are the differences between the OLS sensors and declines in sensor throughput over time. NGDC plans to address the intercalibration of the products through empirical approaches, such as intercomparison of products generated by two or more satellites for the same set of nights and the use of sets of lights deemed to have been stable over time. The nighttime lights products may be useful in modeling the spatial distribution of population density, distributed carbon emissions, and economic activity.

## 1. INTRODUCTION

Since the early 1970's the U.S. Air Force Defense Meteorological Satellite Program (DMSP) has operated polar orbiting platforms carrying Operational Linescan Systems (OLS) capable of detecting clouds using two broad spectral bands: visible and thermal infrared. The program began with the SAP (Sensor Aerospace Vehicle Electronics Package) which were flown from 1970-76. The current generation of OLS sensors began flying in 1976 and are expected to continue flying until ~2010. At night the visible band is intensified with a photomultiplier tube to permit detection of clouds illuminated by moonlight. A digital archive for the DMSP-OLS data was established in mid-1992 at the NOAA National Geophysical Data Center (NGDC). NGDC has had a ten year program to develop algorithms for producing nighttime lights products from OLS data and applications for the products (Elvidge *et al.*, 1997, 2001 and 2003). Since 2000, NGDC has concentrated on producing nighttime lights product suitable for change detection. This paper reviews some preliminary results from the nighttime lights change detection products from 1992 and 2003.

## 2. DATA PROCESSING

The complete set of nighttime OLS data was extracted from the OLS archive and processed to generate geolocated images (30 arc second grids) from the individual orbits in which lights, clouds, and data quality characteristics were identified. Cloud-free data from these images acquired under conditions of zero

lunar illuminance were then composited to form global composites. The raw composites contain light detections from human settlements, gas flares, fires and heavily lit fishing boats. The four types of lighting can then be separated based on the location, appearance, and temporal character of the lighting. The following section briefly outlines the processing algorithms.

### LABELING VISIBLE BAND DATA QUALITY

Processing to label the quality of nighttime lights data in each pixel begins with the calculation of the latitude and longitude of each pixel center using the satellite ephemeris for each scanline. The calculation is done without terrain correction to save time. The latitude/longitude coordinates are held in memory while the sunlit data are identified and lunar illuminance calculations are performed.

### Sunlit Data

The solar elevation angle for each pixel is calculated using equations from Meeus (1991). The calculation uses the year, month, day and time, plus the latitude/longitude for each pixel. Pixels having solar elevation angles greater than -6 degrees were flagged as sunlit. Solar elevation angles are held in memory for use in the glare detection described below.

### Lunar Illuminance

The lunar illuminance for each pixel was estimated with equations from Janiczek and DeYoung (1987) using the same

---

\* Corresponding author.

inputs as the solar elevation calculation. Pixels having zero lunar illuminance were flagged.

## Glare

Images were searched for solar glare, a condition caused when sunlight is scattered into the OLS telescope. Glare is only possible in scanlines where the minimum solar elevation exceeds -40 degrees. Potential glare is detected based on the presence of 75 or more saturated visible band pixels found in 40 by 40 windows tiled through the image. This condition spawns a search for contiguous pixels having DN values greater or equal to 20. The scanlines containing these image sections are then checked to ensure that some portion of the scanline has a solar elevation angle greater than -40 degrees.

## Marginal Data

Pixels are flagged as "marginal" if marginal data if they occur in scanlines with glare or sunlit data. All scanlines located poleward between glare and sunlit data are also flagged as marginal. The marginal data have slightly elevated DN values when compared to the highest quality nighttime lights.

## Bad Scan Lines and Lightning

A bad scan line is defined as a scan line with 10 consecutive lights, with no lights above or below them. This algorithm is run on the flagged lights. This algorithm also detects many of the streaks of light generated when scanlines cross clouds illuminated by lightning. As an additional test applied to F10 data, pixels with at least  $n$  consecutive zero values in the visible band with no zero data above or below are identified as bad scan lines.

## GEOLLOCATION

All images were projected into 30 arc second grids. The geolocation algorithm operates in the forward mode, projecting the center point of each pixel onto the Earth's surface. The geolocation algorithm estimates the latitude and longitude of pixel centers based on the geodetic subtrack of the satellite orbit, satellite altitude, OLS scan angle equations, an Earth sea level model, and digital terrain data. The geodetic subtrack of each orbit is modeled using daily radar bevel vector sightings of the satellite (provided by Naval Space Command) as input into an Air Force orbital mechanics model that calculates the satellite position every 0.4208 seconds. The satellite heading is estimated by computing the tangent to the orbital subtrack. We have used an oblate ellipsoid model of sea level and have used 30 arc second shuttle radar topography mission (SRTM) data as a source of digital terrain elevations.

## CLOUD DETECTION

Cloud detection was performed using the thermal band data. For a number of years NGDC used image analysts to set thermal band thresholds for cloud detection, as described in Elvidge et al. (1997). NGDC has recently implemented an automatic cloud detection algorithm based on differencing the OLS thermal band brightness temperatures with gridded surface temperature values produced by NOAA National Center for Environmental Prediction (NCEP).

In the NCEP surface temperature grids, the grid cell value represents an average surface temperature across the grid cell. In grid cells that have both land and sea contribution, the land/sea boundary is muted in the NCEP grid, but is present in the higher spatial resolution OLS thermal band. This resulted in the inability to accurately detect clouds along coastal boundaries. For example, in coastal grid cells where the land is relatively cooler than the sea, the NCEP surface temperature average across that grid cell would report a warmer temperature and the land would often be misidentified as a cloud. To address this problem, a land-sea lookup table was created for each coastal NCEP grid cell. The lookup table consists of three columns and has for each coastal NCEP grid cell, the nearest NCEP all land grid cell, and the nearest NCEP all sea grid cell. Separate lookup tables were created for the NCEP 1 degree grids and the NCEP 2.5 degree grids.

Each OLS image processed was temporally matched to nearest NCEP surface temperature grid. The NCEP grid was resampled to a 30 arc second grid covering the study area. The coastal look up table was used to re-assign surface temperatures in the 30 arc second cells coming from the 1 degree and 2.5 degree NCEP cells straddling land and water. Then a temperature difference image was generated by subtracting the 30 arc second NCEP derived surface temperatures from the 30 arc second OLS thermal band brightness temperatures. A temperature difference histogram was calculated for all the open water cells from each OLS image. Typically the histogram displays a bell shaped peak at or near the origin, representing data from the cloud-free open water areas. The center of this peak was defined as the maximum peak within 15 degrees of the origin. Half of a Gaussian curve is fit to the data to the left of this peak. In practice this is done by replicating and mirroring the data from the values less than the peak over to the values greater than the peak and fitting a Gaussian. The cloud detection threshold is then the mean plus two standard deviations of this Gaussian, with a further constraint that the thresholds not deviate from the range [5, 20]. That is, the chosen difference threshold must be between 5 and 20 degrees Celsius.

## COMPOSITING

Global composites of the average visible band digital number (DN) were generated using nighttime visible band data meeting the following criteria:

- Zero lunar illuminance.
- High quality visible band data (no glare, marginal, bad scan lines or lighting).
- Cloud-free.
- Center half of swath (better geolocation, sharper light features, more consistent radiometry).

The resulting average visible band DN composites were then further processed to remove background noise and ephemeral lights (e.g. fires). Areas devoid of detected lighting are identified based on their low average visible band DN and low standard deviation. Ephemeral lights are identified based on their high standard deviation and relatively low average visible band DN.

Major flaws in the composites include visible band saturation in major urban centers, undetected snow effects, radiometric differences between sensors, the decline in sensor throughput over time. In addition to these flaws, the areas of detected

lighting are known to overestimate the actual size of lighting on the ground (Imhoff *et al.*, 1997 and Henderson *et al.*, 2003). This area overestimation is due to a combination of factors: the large OLS pixel size, the OLS' capability to detect subpixel light sources, and geolocation errors (Elvidge *et al.*, 2004b). Surface effects, such as the presence of snow cover and the reflection of lighting by near shore waters also contribute to the spread of light that can be detected by the satellite. These effects, present in data from single observations, are accumulated during the time series analysis.

NGDC plans to address the inter-calibration of the products through empirical approaches, such as inter-comparison of products generated by two or more satellites for the same set of nights and the use of sets of lights deemed to have been stable over time.

### 3. RESULTS

A preliminary examination of the nighttime lights time series reveals that nighttime lights can both expand or contract in response to economic conditions. In the USA and many other developed countries, lighting was observed to expand in a rather uniform manner, with rims of lighting growth surrounding major cities and growth in the brightness of lights in many smaller towns. In contrast, lighting was observed to contract in many parts of the former Soviet Union. Figure 1 shows the lighting for Moldova from 1992 and Figure 2 shows the lighting for Moldova from 2003. In 1992 many parts of the country had lighting present. In 2003 only a few large cities had lighting. Rapidly developing countries, such as India and China, exhibit wide regional variation in the level of lighting expansion with localized areas of lighting contraction. Some of these patterns track administrative boundaries, indicating state and provincial differences in economic growth patterns.



Figure 1. Nighttime lights of Moldova from 1992.

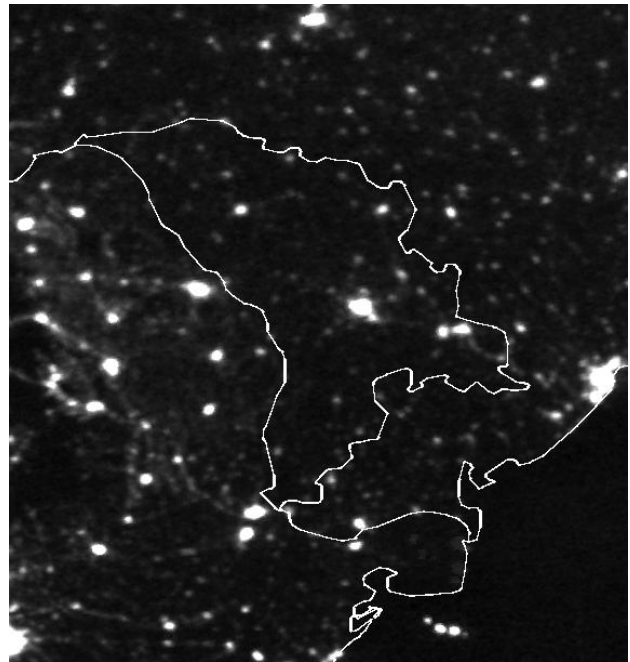


Figure 2. Nighttime lights of Moldova from 2003.

### 4. CONCLUSIONS

NGDC has produced a time series of global nighttime lights products optimized for change detection. The digital method for mapping night-time lights with OLS data utilize large number of orbits to overcome the obscuring effects of clouds and to separate the observed lights into four primary categories: human settlements, gas flares, fishing boats, and ephemeral lights (mostly fires). A preliminary examination of the products reveals that lighting changes are common and can be detected by satellite.

Nocturnal lighting could be regarded as one of the defining features of concentrated human activity. Satellite observations of nocturnal lighting can be viewed as an index of human activity, similar to the red and near infrared vegetation index (VI) or sea surface temperature (SST).

The incredible low-light imaging capabilities provided by the DMSP program are expected to continue until at least the year 2010. The NOAA-DoD converged system of meteorological sensors (NPOESS), scheduled for deployment towards the end of this decade, will preserve the low-light sensing capability initiated with the OLS. Thus, the mapping of light sources present at the earth's surface using night-time satellite data can be expected to be a continuing source of information for the coming decades.

The nighttime lights products have been proven to be useful in the analysis of impervious surface areas (Elvidge *et al.*, 2004b) urban heat islands (Owens *et al.*, 1998), terrestrial carbon dynamics (Milesi *et al.*, 2003), and the modelling of artificial sky brightness (Cinzano *et al.*, 2001) and the spatial distribution of population density (Sutton *et al.* 2001 and 2003). The close linkage between lights, economic activity, and energy related carbon emissions (Doll *et al.*, 2000) indicates that the lights may be useful in independent estimation of national carbon emissions and gross domestic product.

## 5. REFERENCES

- Cinzano, P, Falchi, F., Elvidge, C.D., 2001, The first world atlas of the artificial night sky brightness. *Monthly Notices of the Royal Astronomical Society* 328, pp. 689-707.
- Doll, C.N.H., Muller, J-P., Elvidge, C.D., 2000. Night-time imagery as a tool for global mapping of socio-economic parameters and greenhouse gas emissions. *Ambio* 29, pp. 157-162.
- Elvidge, C.D., Baugh, K.E., Kihn, E.A., Kroehl, H.W, Davis, E.R, 1997. Mapping of city lights using DMSP Operational Linescan System data. *Photogrammetric Engineering and Remote Sensing* 63(6), pp. 727-734.
- Elvidge, C.D., Safran, J., Nelson, I.L., Tuttle, B.T., Hobson, V.R., Baugh, K.E., Dietz, J.B., Erwin, E.H., 2004a, Area and position accuracy of DMSP nighttime lights data. *Remote Sensing and GIS Accuracy Assessment*, CRC Press, pp. 281-292.
- Elvidge, C. D., C. Milesi, J. B. Dietz, B. T. Tuttle, P. C. Sutton, R. Nemani, and J. E. Vogelmann, 2004b, U.S. Constructed Area Approaches the Size of Ohio, *Eos, Trans. AGU* 85(24), p. 233.
- Elvidge, C.D., Hobson, V.R., Nelson, I.L., Safran, J.M., Tuttle, B.T., Dietz, J.B., Baugh, K.E., 2003, Overview of DMSP-OLS and scope of applications. *Remotely Sensed Cities*, Taylor and Francis, London, pp. 281-299.
- Elvidge, C.D., Imhoff, M.L., Baugh, K.E., Hobson, V.R., Nelson, I., Safran, J., Dietz, J.B., Tuttle, B.T., 2001, Nighttime lights of the world: 1994-95. *ISPRS Journal of Photogrammetry and Remote Sensing* 56, 81-99.
- Gallo, K.P., Elvidge, C.D., Yang, L., Reed, B.C., 2003 Trends in nighttime city lights and vegetation indices associated with urbanization within the conterminous USA. *International Journal of Remote Sensing* 25(10), pp. 2003-2007.
- Henderson, M., Yeh, E.T., Gong, P., Elvidge, C.D. Baugh, K., 2003, Validation of urban boundaries derived from global night-time satellite imagery. *International Journal of Remote Sensing* 24, pp. 595-609.
- Imhoff, M.L., Lawrence, W.T., Stutzer, D.C. and Elvidge, C.D., 1997, A Technique for Using Composite DMSP/OLS "City Lights" Satellite Data to Accurately Map Urban Areas. *Remote Sensing of Environment* 61, pp. 361-370.
- Milesi, C., C. Elvidge, R. Nemani and S. Running. (2003) Assessing the impact of urban land development on net primary productivity in the southeastern United States. *Remote Sensing of Environment* 86 pp. 401-410.
- Owen, T.W., Gallo, K.P., Elvidge, C.D., Baugh, K.E., 1998. Using DMSP-OLS light frequency data to categorize urban environments associated with US climate observing stations. *International Journal of Remote Sensing* 19(17), pp. 3451-3456.
- Sutton, P., Elvidge, C., Obremski, T., 2003, Building and evaluating models to estimate ambient population density. *Photogrammetric Engineering and Remote Sensing* 69(5), pp. 545-552.
- Sutton, P., Roberts, D., Elvidge, C., and Baugh, K., 2001, Census from Heaven: an estimate of the global population using night-time satellite imagery. *International Journal of Remote Sensing* 22(16), pp. 3061-3076.